Title: Biotin Engineered HPMA Nanoparticles and Effective Targeting of Bortezomib: *In Vitro* and *In Vivo*

Introduction

In 1970, Ringsdorf first highlighted the use of polymers as a therapeutic agent. Since then, plentiful of literature has been published on polymeric drug delivery [1]. Polymeric conjugates are an astounding approach for the targeted delivery of drugs at tumorous site. These can mask and release the therapeutics/bio-actives at diseased site in control manner. The breakthrough outcome was witnessed when the first polymer entered in the clinical trials [2]. Later on, poly-ethylene-glycol (PEG) based conjugates of proteins [3], antibodies [4] and polymeric micelles of encapsulated or conjugated drugs also entered in various clinical phases of evaluation. Conjugated polymer-based drug delivery through a nanoparticulate approach such as polymeric nanoparticles (PNPs), micelles, liposomes, and dendrimers can efficiently deal with solubility and instability issues of various drug molecules. PNPs are colloidal particles in size range of 10-1000 nm with a potential of prolonged distribution of drugs in the blood [5]. PNPs have a high degree of selectivity based on the size and can deliver the conjugated molecules to the desired site of action.

Breast cancer has been ranked as a second foremost cause of death worldwide among all the cancer subtypes [6]. Despite the advanced chemotherapy that improved the life span of patients, the mortality rate due to cancer has not decreased significantly. One of the reasons sought to be the vague targeting and cytotoxic effects of drugs, which limits as well as hampers the positive effect of chemotherapy. ER-positive subtype is the most commonly diagnosed breast cancer (70%) in women [7]. Bortezomib (BTZ) is a proteasome inhibitor, approved by US FDA (Food and Drug Administration) in 2003 for the treatment of multiple myeloma and have showed outstanding results for solid tumor treatment as a single or combination agent [8, 9]. BTZ have revealed some extraordinary outcomes against ER-positive breast cancer recently [10-12]. But the low aqueous solubility, unstable nature and poor tumor cells penetration are the major drawbacks of BTZ [13]. Su et al. explored the catechol conjugated polymers for BTZ delivery for breast cancer cells (as MDA MB-231, MCF-7). Results suggested that the prepared catechol system may be beneficial in cancer therapy [14]. Medel and coworkers prepared curcumin and BTZ loaded nanoparticles and observed the synergistic effect of curcumin and BTZ nanoparticles against solid tumor [15].

HPMA [N-(2-hydroxypropyl) methacrylamide], a co-polymer has been widely explored for polymeric-drug conjugated delivery by Duncan and co-workers in the last two decades [16]. HPMA, a hydrophilic polymer was supposed to enhance the aqueous solubility of hydrophobic drugs. HPMA gained much attention as its first polymeric conjugate (FCE28068) entered in the clinical trials in 1999 [17]. Considering its attractive properties and its fruitful applicability reports in drug delivery we selected HPMA as a hydrophilic carrier for our protocol. PLA (poly-L-lactic acid) was considered as hydrophobic segment in an anticipation that it will help the encapsulation of hydrophobic drug(s) into the intended PNPs, which is the proposed final formulation in the present study. PLA is also biocompatible and biodegradable in nature which is advantageous for this study. Barz et al. reported paclitaxel loaded HPMA polymeric micelles and studied their intracellular uptake and localization in HeLa cells (Human cervix adenocarcinoma cells). [18]. Surprisingly, there is scarcity of the literature related to HPMA applications in bio-medicals specially the conjugation-oriented strategies [18]. Hitherto, none of them reported a combined ester and amide linkage approach with biotin for developing PNPs with targeting potential. However, large sized particles are easily engulfed by reticular endothelial cells [19] but this shortcoming can be reduced by developing a tumor specific nanoparticulate system such are targeted PNPs proposed in the present study. Significant drug loading is also expected to meet the requirement of suppression of cell proliferation and eventually to kill cancerous cells/tissue. Cancer cells usually have a hunger for some vitamins and receptors [20]. Biotin receptors are highly over expressed in certain cancers subtypes such as breast, lung, ovarian etc. in comparison to normal cells [21]. Among various vitamins, biotin draws special attention as it is being up taken more rapidly by cancer cells than the normal cell [22].

Our hypothesis is based on the conjugation of different copolymers with biotin as a targeting ligand to examine the effect of biotinylated conjugates v/s non-biotinylated conjugates on breast cancer cells **(Figure 1)**. Therefore, the first milestone challenge of this work is to synthesize and characterize the HPMA-PLA conjugates and thereafter tethering the biotin in this co-polymeric structure making it as HPMA-PLA-Biotin. The second milestone challenge is to fabricate the PNPs formulation with optimized encapsulation of BTZ using suitable method. Finally, the last challenge is to evaluate the targeting potential of developed PNPs in breast cancer cells (MCF-7 and MDA MB 231) assessing anti-cancer potential *in vitro* and *in vivo* [10-12, 14-15]. It was also envisaged that conjugation with HPMA can potentiate drug payload and enhanced

the blood residence of drug which in-turn would improve the overall bioavailability of BTZ. Obviously, the hidden/parallel objective was also to improve the solubility of the BTZ using HPMA-PLA based copolymers (data not included) for the better and stable formulation development of BTZ.

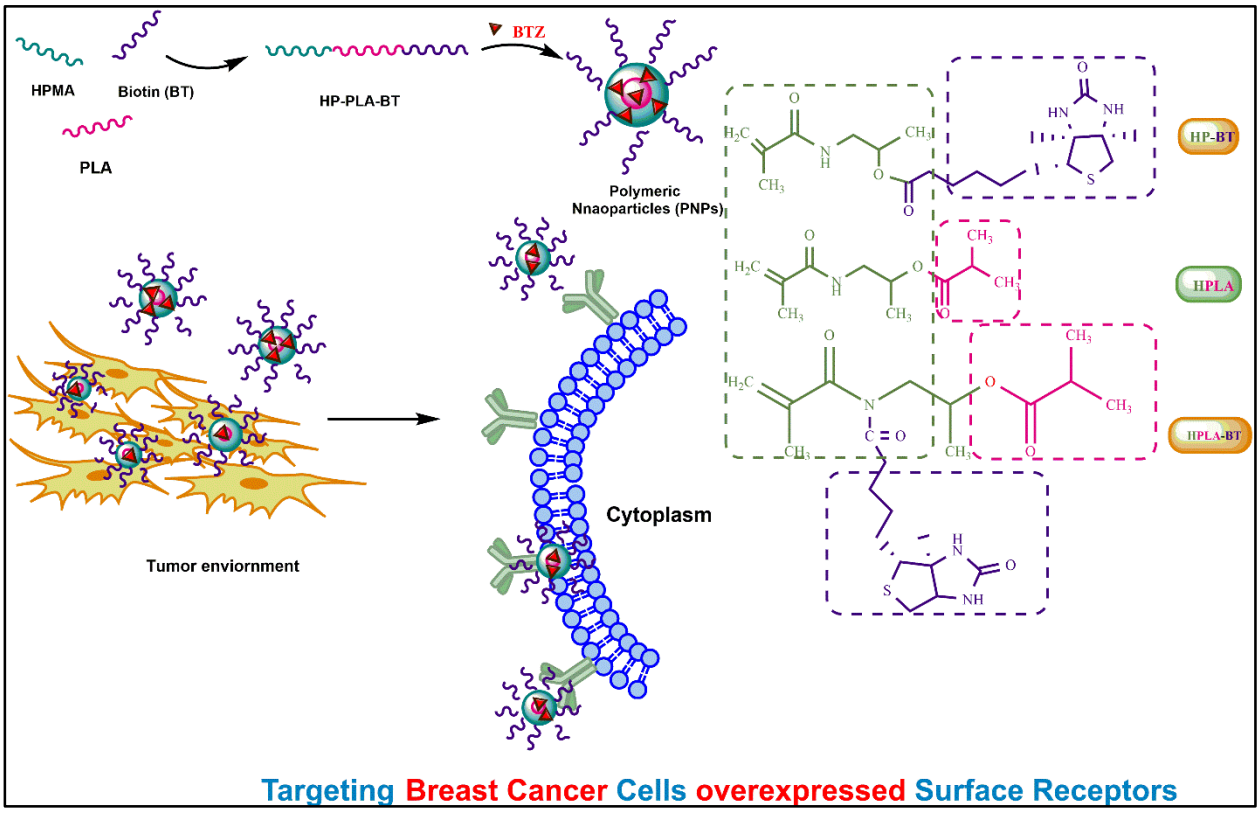

Figure 1: Schematic representation of overall proposed work.

Specific Objectives

The foremost objective of the proposed work was targeted delivery of BTZ encapsulated polymeric nanoparticles to the intended tumorous site. HPMA based polymeric conjugates have the capability to enhance the drug efficacy to a greater extent. The main purpose of this work was to deliver BTZ by conjugating biotin (ligand) that provided drug delivery in targeted manner and sustained effect for the better treatment of breast cancer. The following were the specific objectives to address

- ❖ Design, synthesis, and characterization of HPMA-Biotin, HPMA-PLA, and HPMA-PLA-Biotin polymeric conjugates (FT-IR, NMR).
- ❖ Preparation and characterization of BTZ encapsulated PNPs of the above synthesized copolymers.

- *In vitro* and *in vivo* evaluation of PNPs including release kinetics, hemolytic toxicity, cytotoxicity, pharmacokinetics etc.

Materials and Methods

Materials

Methacryloyl chloride, aminopropanol-2-ol were procured from Alfa-Aesar Pvt. Ltd. India. Anhydrous sodium carbonate, anhydrous sodium sulfate, dry dichloromethane (DCM), acetone, methanol (MeOH), thionyl chloride ($SOCl_2$), chloroform, dimethyl sulfoxide (DMSO), tetrahydrofuran (THF), triethylamine (TEA) were purchased from TCI Chemicals Pvt. Ltd. India. PLA (molecular weight 10000-18000 Da) was a gift sample from Evonik Industries. Biotin, 4-dimethyl aminopyridine (DMAP), MTT (3-(4,5-dimethylthiazol-2-yl)-2,5-diphenyl tetrazolium bromide), FITC (fluorescein isothiocyanate), DMEM (Dulbecco's Modified Eagle Medium), FBS (fetal bovine serum), streptomycin-penicillin, trypsin EDTA, dialysis membrane-50 and 150 were purchased from Hi-Media and were used as such without any further purification. N, N-dicyclohexyl carbodiimide (DCC), 1-ethyl-3-(dimethylaminopropyl) carbodiimide (EDC), polyvinyl alcohol (PVA), lecithin, disodium hydrogen phosphate, potassium dihydrogen phosphate, tetrahydrofuran (THF), sodium hydroxide, sodium chloride, and ethanol were obtained from CDH, India. TLC plates were procured from Merck, India. Whatman filter papers and syringe filters were procured from Rankem, India. All the other reagents were of analytical grade with highest purity.

SYNTHESIS AND CHARACTERIZATION POLYMERIC CONJUGATES

Synthesis of HPMA (N-2-hydroxypropylmethacrylamide) and its conjugates such as HPMA-Biotin (HP-BT), HPMA-PLA (HPMA-poly-L-lactic acid; HPLA) and HPLA-Biotin (HPLA-BT)

HP-BT (N-2-hydroxypropylmethacrylamide-Biotin or HPMA-Biotin)

First, the co-polymer HPMA was synthesized according to previously reported literature [24]. HPMA (HP) and biotin (BT) were conjugated using DCC/DMAP coupling reaction. Briefly, HP (10 mg) was dissolved in DCM, then added into the BT solution (25.44 mg in DMSO) followed by addition of DCC. After 20 min, DMAP (dissolved in DCM) was added slowly to the reaction mixture and reaction time allowed was 24 h. TLC was performed to examine the initially to

confirm the completion of reaction. The crude product was vacuum dried and kept in dialysis bag after dissolving in distilled water. The whole assembly was stirred in distilled water for 2 days to remove DMAP impurities from the product. The external solvent (water) was replaced after 12 h timely. After that, a brown colored product was dried and a yield of 86% was calculated. The conjugate was characterized at each step by FT-IR and NMR spectroscopy.

HPLA (HPMA-Poly-L-lactic acid)

HPMA was conjugated to PLA according to the reported procedure [25]. Poly-L-lactic acid (PLA) (500 mg, 0.05 mmol) was dissolved in DCM (5 mL) with HPMA (7.1 mg, 0.05 mmol) in the excess of DCC (10.31 mg, 0.05 mmol). After 20 min, DMAP (6.1 mg, 0.05 mmol) was added to the reaction mixture. The reaction was allowed to proceed overnight. The conjugate was dialyzed using dialysis membrane for 24 h to remove DMAP. HPLA co-polymer was characterized by FT-IR using KBr pellet method (Perk, M/s Perkin Elmer Co., Waltham, Massachusetts, USA) and ^{1}H–NMR spectra were recorded in Bruker Ascend 500 MHz NMR spectrometer (Switzerland) using $CDCl_3$ as the solvent.

HPLA-BT (HPMA-Poly-L-lactic acid-biotin conjugate)

Biotin (BT) (100 mg) was dissolved in dry DCM (5 mL) in RBF and kept at 0 ºC. Thionyl chloride (59.38 μL) was added dropwise into the above solution. Thereafter, the reaction was transformed at 60 °C for 4-6 h. On completion of reaction, flask was cooled at room temperature and a solid yellow brown colored product was obtained. The product was washed three times with chilled DCM and vacuum dried [26]. The product was immediately used for the next reaction. This biotin acylchloride (BT-Cl) intermediate was vacuum dried and further conjugated to HPLA. In the next step, HPLA (207 mg) was dissolved in dry DCM and kept for stirring at 0 ºC. Then, tertiary amine (Et_3N) was added to the reaction dropwise. Later, dry THF was added in the reaction mixture and reaction was allowed to proceed in cool conditions and in inert atmosphere for 18-20 h [27-28] Subsequently, the product was dissolved in cold DCM (dichloromethane) and dried. The obtained product was washed with chilled DCM to remove the remaining traces of unreacted/unmodified HPLA. The co-polymeric conjugate (HPLA-BT or HPMA-PLA-BT conjugate) was obtained as yellow color solid. Finally, the product was characterized by ^{1}H and ^{13}C-NMR spectroscopy.

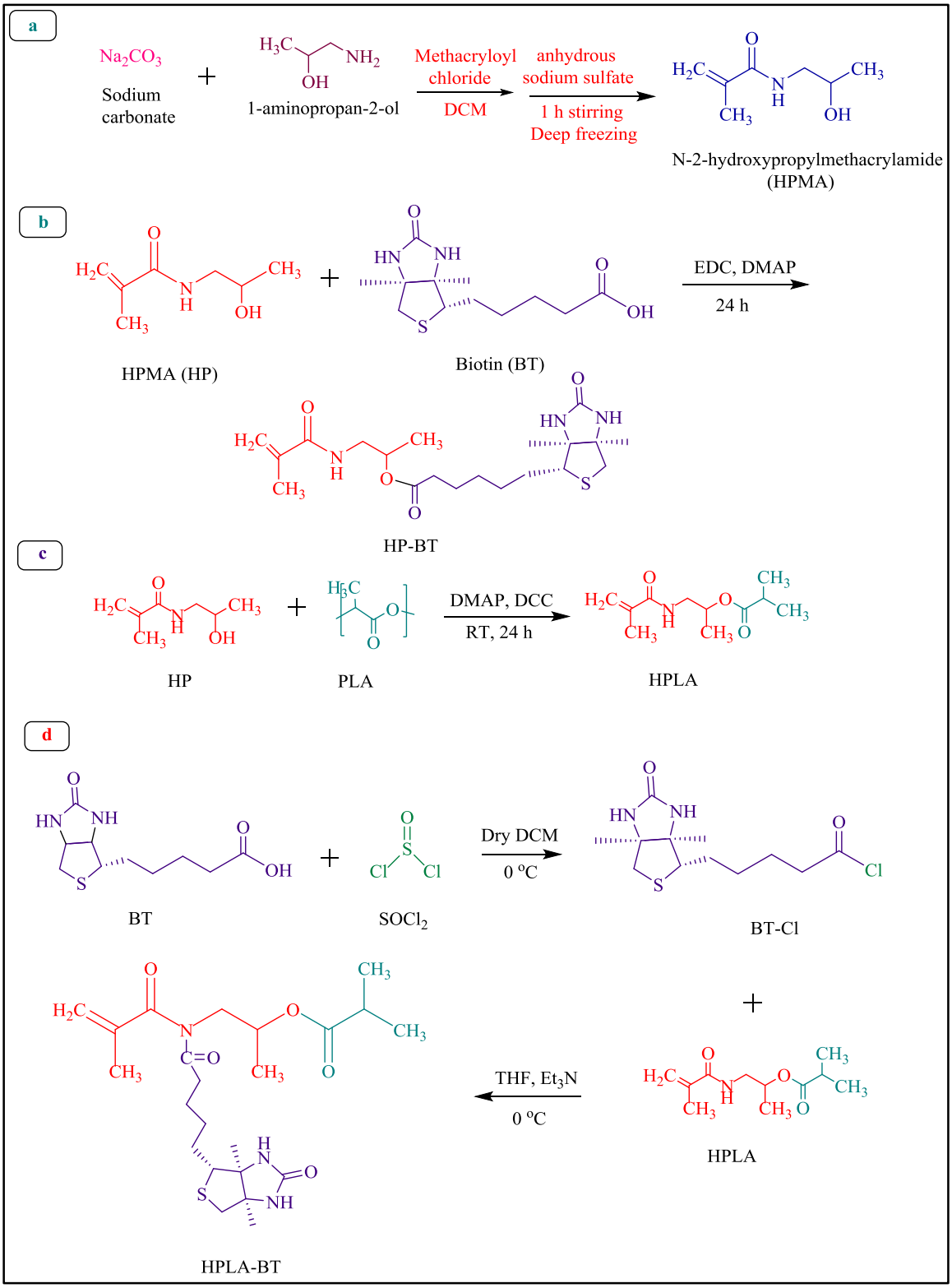

Figure 2: Synthesis schemes of; (a) HPMA (b) HPMA-Biotin (HPBT) (c) HPMA-PLA (HPLA) (d) HPMA- PLA-Biotin (HPLA-BT).

Preparation of HP-BT, HPLA, HPLA-BT polymeric nanoparticles (PNPs)

The prepared polymeric conjugates (HPBT, HPLA, HPLA-BT) were used for the fabrication of BTZ loaded PNPs. Following the o/w single emulsification method [29], weighed co-polymeric conjugates (10 mg) were dissolved in 5 mL of DCM, separately. Then, 1% w/v PVA (polyvinyl alcohol) solution was dissolved in distilled water and added to the co-polymeric solution. BTZ was dissolved in methanol and lecithin solution (4% ethanol and heated at 65 ºC) were added dropwise (1 mL/10 min) under magnetic stirring with a homogenous speed to the above mixture. The reaction vessel was left for stirring to completely get rid of organic solvent. Finally, the nanoparticles were vortexed for 5-7 minutes and were dialyzed using dialysis membrane (MWCO 10 kDa) for the entire day. The PNPs solution was collected, lyophilized, and stored at -20 ºC for further use [30]. In total, three blank PNPs i.e. HPBT, HPLA, HPLA-BT and three BTZ loaded PNPs i.e. DL-HPBT, DL-HPLA, DL-HPLA-BT were prepared successfully.

Characterization of HPLA-BT PNPs

^{1}H-NMR Spectroscopy

^{1}H-NMR spectrums were recorded to discriminate the blank and drug loaded PNPs. All the samples were dissolved in D_2O (deuterated) solvent and processed in 500 MHz NMR spectrometer.

Particle size, zeta potential, PDI (polydispersity index)

The prepared HPLA-BT PNPs and other polymeric conjugates were characterized by zeta sizer Nano ZS (Malvern Instruments, Malvern, UK) for particle size, zeta potential and PDI. Zeta sizer is based on the principle of photon correlation spectroscopy (PCS) where the average particle size was calculated by measuring the wideness of particle size distribution. The PNPs were suspended in 1 mL deionized water and filtered the solutions by syringe filter (0.22 μm) before measurement. Results were expressed as triplet of mean ± SD.

Surface morphology (Atomic Force Microscopy; AFM)

Microscopy was performed using AFM technique for surface characteristics. For AFM analysis, fresh samples were prepared by dispersion of PNPs in double distilled water. The dried thin film of samples was spread over the silicon wafer using the spin coating phenomenon. Silicon wafer were dried, and excess of water was drawn off using filter paper. The results were recorded using Bruker nanoscope V software and images were taken with 256 x 256-pixel camera, and 300 Hz cantilever frequency after measuring the various sections of thin film samples. Ra (average

roughness value), Rq (root mean square roughness defined the surface texture and kurtosis value says about the bumpy, spiky, and perfectly random surface [31].

Drug loading capacity (DLC) and drug entrapment efficiency (DEE)

The drug loading capacity of prepared PNPs (i.e. DL-HPBT, DL-HPLA, and DL-HPLA-BT) was determined by membrane dialysis method. Nanoparticles suspension (2 mL) was filled in dialysis bag (MWCO 5 kDa, Hi-media Laboratories Pvt. Ltd., Bangalore, India) and dialyzed against perfect sink condition for 2 h to allow the unentrapped drug drawn off from the dialysis bag. The amount of unentrapped drug was analyzed at 270 nm using HPLC. The % DEE and % DLC was calculated using the mentioned equations.

$$\% \text{ DEE} = \frac{\text{Total drug feed} - \text{Amount of unentrapped drug}}{\text{Total drug feed}} \times 100$$

$$\% \text{ DLC} = \frac{\text{Total drug feed} - \text{Amount of unentrapped drug}}{\text{Total polymer feed}} \times 100$$

HPLC (High performance liquid chromatography)

BTZ estimation during release and other biological studies was performed using reverse phase HPLC analysis. The reverse phase HPLC (RP-HPLC) analysis was performed at Central University of Rajasthan, Ajmer. The HPLC system used was Shimadzu LC-2010 CHT (Tokyo, Japan) with PDA detector. Merck HPLC column (RP C_{18} 18, 4.6 mm × 250 mm) throughout the analysis. The mobile phase utilized consisted of HPLC grade acetonitrile (ACN), water and formic acid (HCOOH) in 70:30:0.1 % v/v, respectively. The flow rate and temperature were maintained to be 1.0 mL/min and 25 $^{\circ}$C, respectively. The area under curve of the samples was analyzed at 270 nm [32, 33].

***In vitro* release and kinetic models**

Time dependent release of BTZ from prepared polymeric nanoparticles were performed in buffer solutions at pH 7.4 and pH 5.6 mimicking the physiological conditions of blood and endosomes, respectively. Briefly, 2 mL suspension of the developed nanoformulation was filled in a dialysis bag (MWCO 5 kDa, Hi-media Laboratories Pvt. Ltd., Bangalore, India) and immersed in 100 mL of PBS under stirring condition of 150 ± 40 rpm. Two milliliters of aliquots were withdrawn at defined time intervals and the same amount of PBS was replenished into the beaker to maintain sink conditions throughout the release study protocol. Similar protocol was followed to obtain the

in vitro release data at pH 5.6 using buffer solution of pH 5.6 as release media. The drug released from formulations was estimated using HPLC method as mentioned earlier. Further, kinetic models were applied to recognize the finest fitted model, different non-linear kinetic models such as, zero order, first order, Higuchi, Korsmeyer-Peppas and Hixson Crowell model for the prepared formulations.

Hemolytic toxicity study

The hemolytic toxicity of BTZ, DL-HPBT PNPs, DL-HPLA PNPs, and DL-HPLA-BT PNPs was performed in concentration dependent manner [35]. The whole blood was collected from a healthy volunteer and stabilized by EDTA. The plasma was removed after centrifugation at 1250 rpm (R-4C DX, REMI, India) for 10-15 min. The collected RBCs were washed twice using normal saline (0.9% w/v) and finally, diluted in 1:10 ratio with normal saline. RBCs suspension (0.8 mL) was mixed with 3.2 mL of the test solutions to make the final concentration 10, 50, 100 and 150 µg/mL. Distilled water and normal saline were regarded as the positive and negative control, respectively. The cell suspensions were incubated for 2 h, and centrifuged. The extracted supernatant was analyzed at 540 nm using UV-visible double spectrophotometer (Perkin Elmer). The percentage hemolysis was calculated using the following equation.

$$\% \text{ Hemolysis} = \frac{\text{Absorbance of test} - \text{Absorbance of negative control}}{\text{Absorbance of positive control} - \text{Absorbance of negative control}} \times 100$$

Cytotoxicity study

The cytotoxicity of BTZ, DL-HPBT PNPs, DL-HPLA PNPs, and DL-HPLA-BT PNPs was evaluated by MTT assay against MCF-7 breast cancer cells [36]. The cell lines were grown in culture media DMEM (Dulbecco's Modified Eagle's Medium) containing 10% v/v FBS (Fetal bovine serum) and 1% v/v L-Glutamine-Penicillin-Streptomycin solution. The cells were seeded uniformly at a density of 1×10^4 cells per well into 96-well plates and incubated overnight in CO_2 incubator (Heracell 150i, Thermo Fisher). After 90% confluency, the cells were treated with different concentration range of formulations and incubated for 24 h (considered complete media as control). Next day, the cells were removed and washed thrice with PBS and to each well 50 µL of MTT solution was added and left for another 4 h incubation. Later, 150 µL dimethyl sulfoxide (DMSO, HPLC grade) was mixed into each well to dissolve the formazan crystals and a violet

color appeared in each well. The absorbance was taken at 570 nm using ELISA plate reader (Omega Fluostar) after incubated 10 min. The IC_{50} values were determined using Microsoft Excel.

Cellular uptake study

In order to investigate the cell uptake potential of prepared formulations, cellular uptake study was performed utilizing fluorescein isothiocyanate (FITC) labeling of MCF-7 cells [37]. The prepared formulations were labelled with FITC (2 mg/mL) via FITC tagging reaction to examine the cell uptake by different drug loaded PNPs formulations (i.e. DL-HPBT PNPs, DL-HPLA PNPs, and DL-HPLA-BT PNPs). Weighed, 2.5 mg of FITC and dissolved in 1 mL of acetone. Then, in a 25 mL RBF, 1 mL of PBS buffer of pH 7.4 was mixed with FITC solution and stirred it, after 30 min drug loaded formulations were added. The reaction was carried out in dark condition for 24 h. For study purpose, MCF-7 cells (4×10^4 cells per well) were seeded in a 6-well plate and incubated overnight. Next day, the culture media was removed from each well and then the cells were treated with FITC (2 mg/mL) tagged formulations diluted with culture media and transferred the prepared formulations into each well for predetermined time interval of 2, 4 and 24 h. FITC treated cells were considered as control for this experiment. The images were captured under OLYMPUS CKXF3 fluorescence microscope using 10 and 40x magnifications.

***In vivo* pharmacokinetic study**

All the animal experimentations performed were approved by the Institutional Animal Ethical Committee, Rungta College of Pharmaceutical Sciences and Research, Raipur, India. *In vivo* pharmacokinetic studies were performed on healthy unisex Sprague Dawley rats weighing 250-300 gm [38]. All the animals were kept on standard diet and water before start of experiment. The animals were divided into four groups, in which each group was comprised of 4 animals. The different group of animals were administered intravenously with BTZ concentration (1 mg/mL), DL-HPBT PNPs, DL-HPLA PNPs, DL-HPLA-BT PNPs in 1 mg/kg equivalent dose of BTZ in sterile water. At defined time intervals, 0.2 mL of blood sample was withdrawn from the retro orbital plexus and collected in a heparin (anti-coagulant) coated vial. The supernatant was withdrawn after centrifugation of the sample withdrawn at 3000 rpm (R-4C DX, REMI, India). And 0.5 mL of acetonitrile was added into each sample and centrifuged immediately to denature blood proteins for better analytical outcomes. The concentration of the supernatant was evaluated at 270 nm by reverse phase HPLC (Shimazdu LC-2010C, Japan) methods explained earlier. The plasma concentration-time graph was plotted using the obtained data and various pharmacokinetic parameters were estimated utilizing one compartment open body model (1 CBM) for *iv* push.

RESULTS

Synthesis and characterization

HPMA (N-2-hydroxypropylmethacrylamide)

HPMA co-polymer was synthesized following a previously reported protocol [24]. A white crystalline product with percent yield of 82% was characterized by spectroscopy techniques.

HPMA-Biotin (HP-BT)

HPMA was further conjugated to BT *via* DCC/DMAP coupling reaction as shown in synthesis scheme (**Figure 2**). In the FT-IR spectrum, peaks were seen at 3443.35 (-CONH), 2861.8 (alkane), 2925.6 (alkene), 1630.62 cm^{-1} (-NH), which indirectly confirmed synthesis. Peaks at 1271.1 and 1039.9 cm^{-1} were of the chemically conjugated moiety ester, which confirmed the conjugation **(Figure 3)**. In the ^{1}H-NMR spectra, δ ppm: 8.14 [-NH, HPMA (d)], 3.09 [t, -CH, HPMA (e)], 5.23 [s -CH_2 (b)], 2.21 [m -CH (H)], 1.23 [m -CH (K)], 2.74 [-CH2 (M)] were observed. **Figure 4 (a)**. Further confirmation was ensured by ^{13}C-NMR (500 MHz, $CDCl_3$) δ ppm: 69.98 [CO (M)], 46.1 [C-N (N)], 172.0 [CO (P)], 140 [C (R)], 168.5 (OCO, HPBT), 22.5 [CH_2 (K)], 41.0 [CH_2 (e)], 161.85 [CO (C)], 29.0 [CH_2 (I)].

HPLA (HPMA-PLA conjugate)

HPMA-PLA conjugation was confirmed by; ^{1}H NMR (500 MHz, $CDCl_3$) δ ppm: 5.13 [m, CH, PLA (a)], 3.61[CH_2 (g)] 1.10 [s-CH_3 PLA (c)], 1.50 [t-CH_3 PLA (f)], 8.26 [s-NH (d)], 1.92 [s-CH_3 (e)] **Figure 4 (b)**. ^{13}C NMR (500 MHz, $CDCl_3$) δ ppm: 169.3 [CO, PLA (a)], 69.0 [CH, PLA (e)], 16.6 [CH_3, PLA (b)], 30.0 [s-CH_3 (d)], 52.5 (CH_2 (c)]. Likewise, the FT-IR peaks at 1630.98 (alkene), 333.94 (1º NH), 2930.42 (=CH; alkene), 1720 cm^{-1} (ester) wavenumbers confirmed peak for conjugation of HPMA and PLA **(Figure 3)**. Before conjugation, the identity of the procured PLA was also confirmed through NMR spectroscopy.

HPLA-BT (HPMA-PLA-Biotin)

The conjugation was ensured by ^{1}H and ^{13}C NMR spectroscopy at each step. ^{1}H NMR (500 MHz, DMSO) δ ppm: 9.64 [-NH, BT (a)], 4.43 [m -CH (b)], 1.13 [m -CH (e)], 1.53 [s CH3 (f)], 3.26 [d CH (d)], 2.94 [CH2 (c)] **Figure 4 (c)**. ^{13}C NMR δ ppm: 162.99 [CO (a)], 22.99 [CH3 (b)], 14.13 [CH3 (c)], 23.34 [CH2 (d)], 53.32 [CH2 (e)], 77.85 [m CH (f)]. FT-IR spectrum peaks at 3453.60 (CONH), 1640. 11 (1º NH; biotin), 605.79 (=C-H), 1725.70 and 1005.64 cm^{-1} (ester peak) suggested the conjugation of HPLA with biotin. The intermediate biotin chloride (BT-Cl) was also

characterized spectroscopically by ^{1}H and ^{13}C NMR analysis to confirm synthesis. All the results comprised and were in favor of synthesis/preparation of polymeric conjugates.

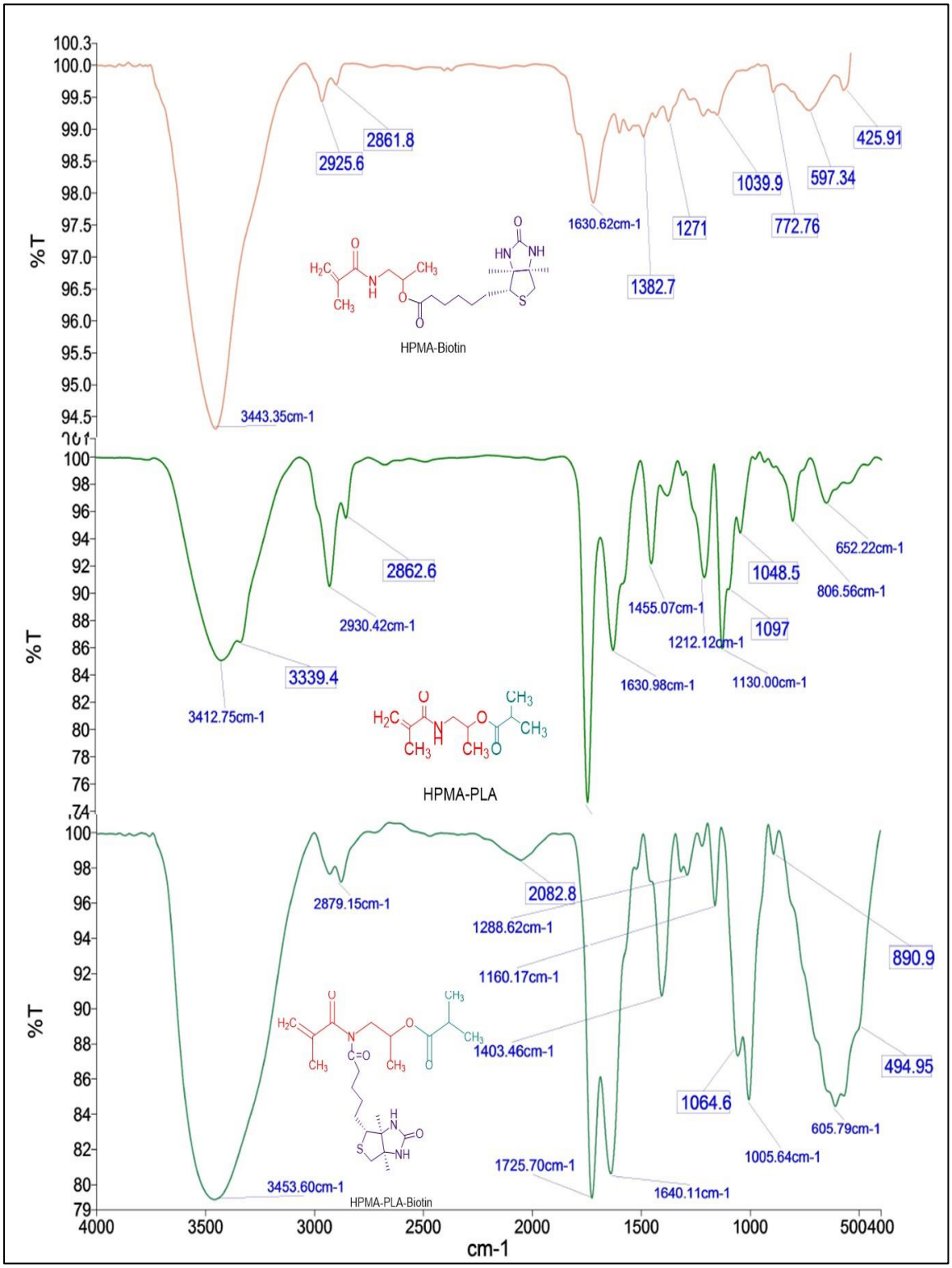

Figure 3: FT-IR spectrum of prepared conjugates: HPBT, HPLA, HPLA-BT. The samples were prepared though KBr pellet method.

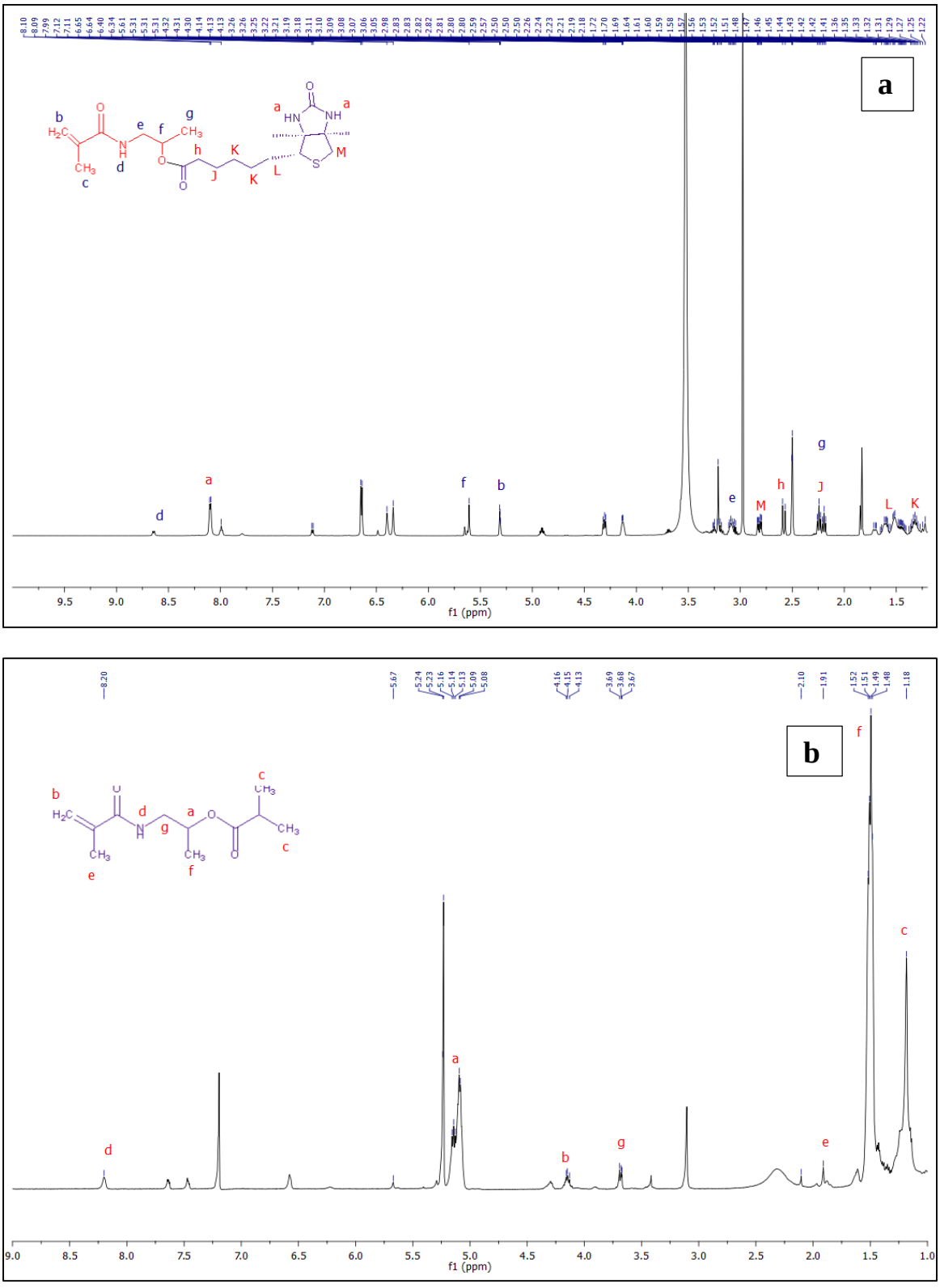

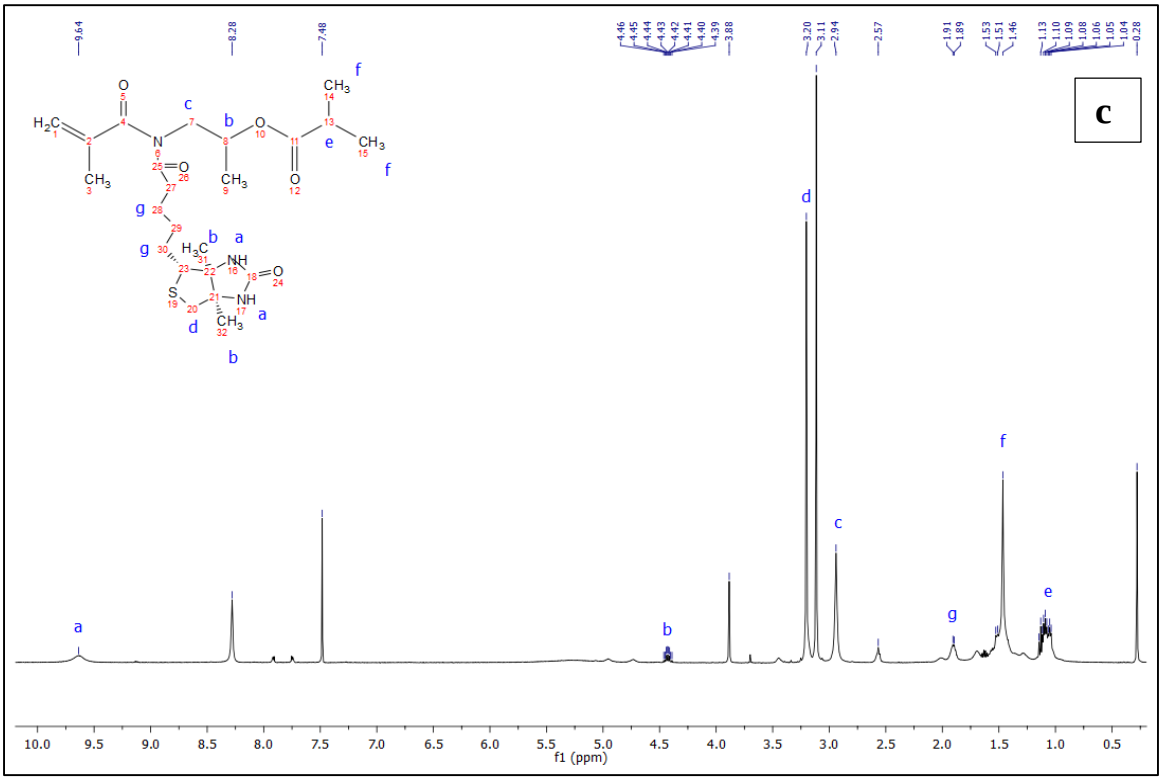

Figure 4: ^{1}H-NMR spectrum (a) HPBT (b) HPLA (c) HPLA-BT.

UV visible spectroscopic characterization of conjugates

UV Visible spectrophotometry was performed for drug as well as all the conjugates. The peaks were clearly visible for biotin around 350 nm. This characterization step further supported the synthesis of HPBT and HPLABT. Maximum absorption is shifted towards longer wavelength **(Figure 5)** in case of DL-HPLA-BT PNPs due to the presence of carbonyl bond in the polymeric conjugate. BTZ absorption can be observed at 300 and 310 nm wavelengths. However, the blank polymeric conjugates showed a less intensified absorption and the overlapped wavelengths were not able to detail any clear indication. The maximum absorption of DL-HPLA-BT PNPs was an indication of conjugation of HPLA with BT and forming a carbonyl bond elucidated as characteristic peak in UV-visible graph.

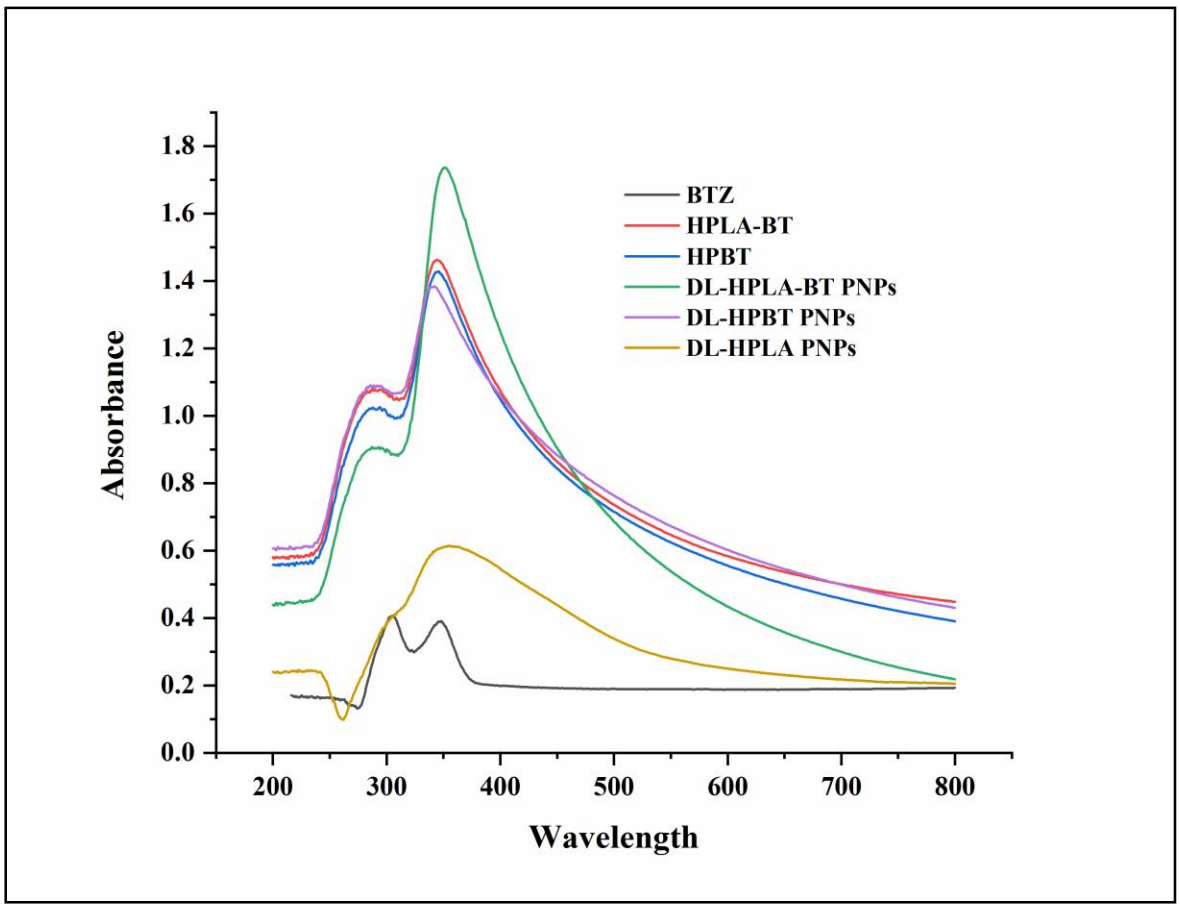

Figure 5: UV-visible spectra of BTZ, HPLA-BT, HPBT and drug loaded (DL); DL-HPLA-BT PNPs, DL-HPBT PNPs, DL-HPLA PNPs, respectively.

Preparation and characterization of PNPs

Polymeric nanoparticles (PNPs) were prepared by o/w single emulsion method particularly to control or optimize the size and drug efficiency of nano-formulations. Finally, the three different formulations i.e. BTZ loaded HPLA PNPs (DL-HPLA), BTZ loaded HPLA-BT PNPs (DL-HPLA-BT) and BTZ loaded HPBT PNPs (DL-HPBT) were prepared, characterized and evaluated in further steps for different outcomes and anticancer activities.

Drug loading capacity (DLC) and drug entrapment efficiency (DEE)

The DLC of DL-HPLA-BT PNPs, DL-HPLA-PNPs and DL-HPBT were found to be 19.73±0.03, 17.93±0.12, 14.75±0.13%, respectively. DEE of DL-HPLA-BT, DL-HPLA and DL-HPBT PNPs were calculated to be 82.20±0.14, 74.68±0.08, 83.59±0.05%, respectively. A slight increase in the DLC was seen in DL-HPLA-BT PNPs as compared to DL-HPLA-PNPs. In the similar way, DEE of DL-HPLA-BT PNPs was higher than HPLA-PNPs **(Table 1)**. The observed slight increase in

the encapsulation can be seen probably due to surface engineering of the HPLA conjugates with biotin (BT) which might be giving more room for encapsulation within respective PNPs.

Table 1: Particle size, zeta potential, drug loading capacity (% DLC) and drug entrapment efficiency (% DEE) of the prepared formulations.

PNPs Code	Size (nm)	Zeta potential (mV)	PDI	Entrapment efficiency (% DEE)	Drug loading (% DLC)
HPBT	213.6±0.25	-7.64±1.23	0.150±3.02	---	---
DL-HPBT	279.7±2.21	-1.07±1.28	0.131±0.22	83.59±0.05	14.75±0.13
HPLA	356.3±2.21	-2.47±0.56	0.254±0.24	-----	-----
DL-HPLA	430.5±2.21	-17.78±0.12	0.269±0.13	74.68±0.08	17.93±0.12
HPLA-BT	185.3±0.21	-6.50±1.12	0.287±0.02	----	-----
DL-HPLA-BT	199.7±1.32	-3.20±0.22	0.196±0.11	82.20±0.14	19.73±0.03

^{1}H-NMR analysis for BTZ loaded formulations

The ^{1}H-NMR spectra showed a difference between PNPs (blank polymeric nanoparticles) and drug loaded-PNPs (DL-PNPs). A sharp peak was noticed at a chemical shift of 3.31 ppm in DL-HPLA-BT PNPs, which is due to the hydrogen atoms attached to the carbon group near to boron atom in BTZ structure while this peak was absent in B-HPLA-BT PNPs. These results indicated the encapsulation of BTZ in DL-HPLA PNPs.

Particle size, zeta potential, PDI (polydispersity index) and microscopy

The followed strategy yielded mean particle size of formulations such as DL (drug loaded or BTZ loaded)-HPLA-BT PNPs, HPLA-BT PNPs, DL-HPLA PNPs, HPLA PNPs, DL-HPBT PNPs and HPBT PNPs 199.7±1.32, 185.3±0.21, 430.5±2.21, 356.3±2.21, 279.7±2.21, 213.6±0.25 nm, respectively in a narrow size range **(Table 1)**. The size can have major impact in drug targeting to tumors as the tumor vasculature cut-off size band varies from 100-800 nm [22]. So, the size of the nanocarriers can be controlled to deliver through the efficacious EPR-mediated therapy. The results obtained for particle size suggested that the DL-HPLA-BT PNPs size lies in 200 nm range that may be helpful for tumor targeting [39]. The small size particles can enter in the tumor cells effortlessly and can produce drug action with a great extent. The size, zeta potential, PDI, % DLC,

% DEE of formulation were tabulated in **(Table 1)**. The prepared PNPs exhibited negative zeta potential which might be due to the presence of ester groups in HPBT, HPLA and HPLA-BT.

Surface morphology evaluation by atomic force microscopy (AFM)

The surface morphology of PNPs was observed by atomic force microscopy (AFM). AFM was performed only for DL-HPLA-BT PNPs which described the surface topography and texture of these PNPs. The surface roughness (Ra) 27.2 nm, root mean square roughness (Rq) 20.2 and skewness 0.168 were observed during analysis. The high kurtosis value of 4.37 has given the idea of spiky surface or high-pitched peak surface for DL-HPLA-BT PNPs [40]. The overall AFM results concluded that the PNPs showed surface roughness with heighted peaks **(Figure 6)**.

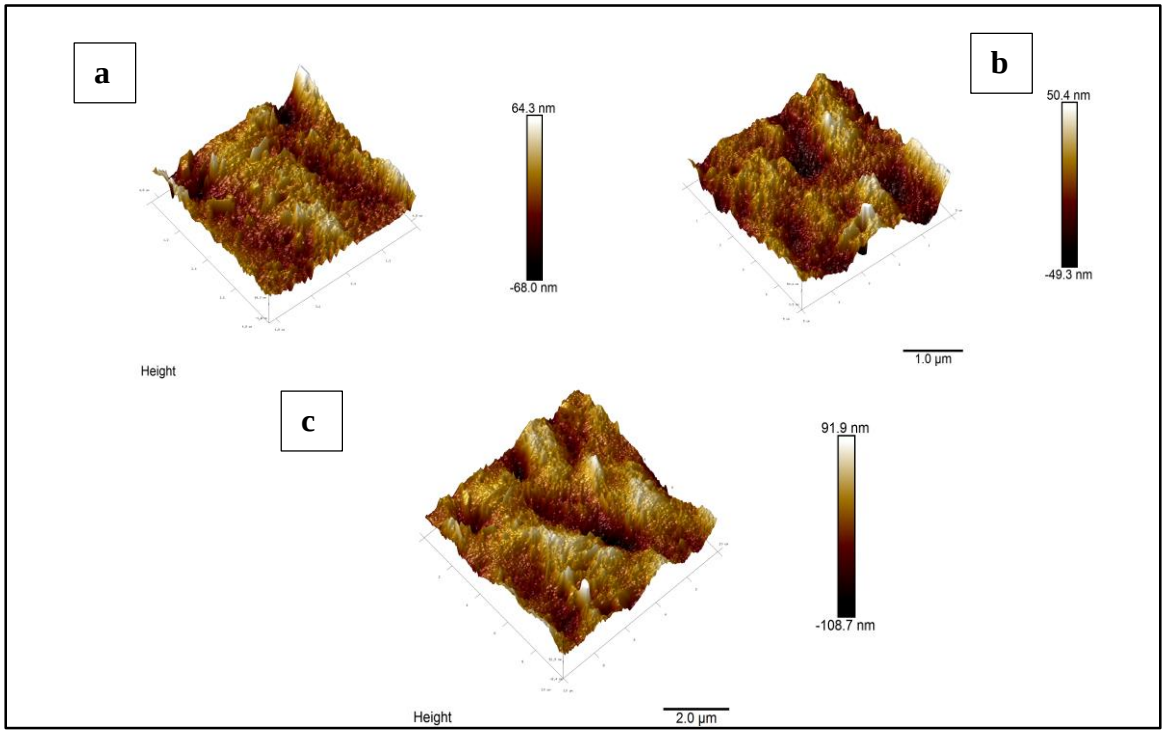

Figure 6: Atomic force microscopy (AFM) of DL-HPLA-BT PNPs. The scale bar of 1.0 µm in image (a) and (b) and 2.0 µm in image (c) represented.

***In vitro* release and kinetic models**

Drug release profile is the key determinant factor to know about the therapeutic performance of a drug in delivery system. At pH 7.4 approximately 55% and 34% of BTZ was released from DL-HP-BT PNPs and DL-HPLA-BT PNPs, respectively in 4 h **(Figure 7 a)**. Similarly, >80% of BTZ was released from DL-HP-BT PNPs, and approximately 76% drug was released from DL-HPLA PNPs while DL-HPLA-BT PNPs released more than 65% of BTZ in 24 h of time point. The obtained results suggested that DL-HPLA-BT PNPs owed slow, and controlled release pattern than

DL-HP-BT PNPs and DL-HPLA PNPs. The controlled release of drug could be beneficial to maintain an appropriate drug concentration in the tumor cells for a prolong period of time so as to improve the overall drug action. These results gave an idea that the drug was encapsulated in the hydrophobic core of nanoparticles and showed a controlled released slowly at pH 7.4 **(Figure 7 a)**. At pH 5.6 **(Figure 7 b)** >50% of BTZ was released from DL-HP-BT PNPs and approximately 45% DL-HPLA PNPs, while it was less than 40% for DL-HPLA-BT PNPs in 4 h. More than 80% drug was released from DL-HPLA-BT PNPs in 10 h. Conclusively, faster drug release was noticed at pH 5.6 for the DL-HPLA-BT PNPs than at physiological pH. The pH 5.6 may be favorable for inducing significant anti-cancer effect of BTZ as tumorous environment is acidic in nature. Different kinetic equations were tested to get a better fit kinetic model in the prepared formulations at pH 7.4 and 5.6. Incorporating the obtained release data into the mentioned kinetic model, the best fit models at pH 7.4 for DL-HPLA-BT PNPs was found to be Korsmeyer-Peppas model (R^2= 0.98), Higuchi model (R^2= 0.95) and first-order model (R^2= 0.93). In case of DL-HPLA PNPs, first-order model (R^2= 0.92), Higuchi model (R^2= 0.94), Korsmeyer-Peppas model (R^2= 0.90) and for DL-HPBT PNPs, first-order model (R^2= 0.93), Higuchi model (R^2= 0.91), Korsmeyer-Peppas model (R^2= 0.90) were the best fit models. At pH 5.6 the best fit models for DL-HPLA-BT PNPs were seen to be Higuchi model (R^2= 0.91), first-order model (R^2= 0.90), Korsmeyer-Peppas model (0.94) and zero-order model (R^2= 0.92). For DL-HPLA PNPs the observations were Higuchi model (R^2= 0.94), first-order model (R^2= 0.92), Korsmeyer-Peppas model (0.91) and zero-order model (R^2= 0.96). For DL-HPBT PNPs the observations were Higuchi model (R^2= 0.95), first-order model (R^2= 0.96), Korsmeyer-Peppas model (0.94) and zero-order model (R^2= 0.98).

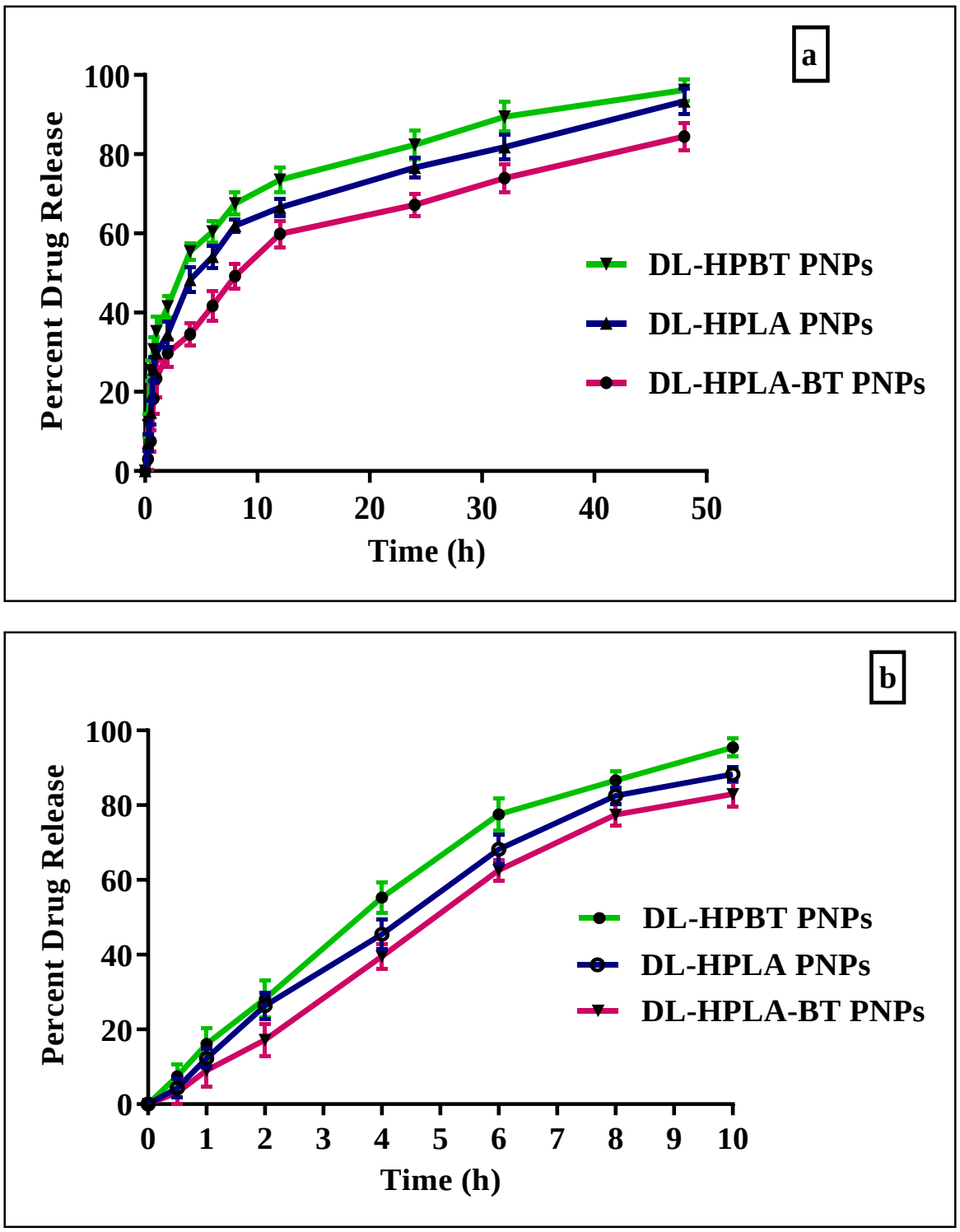

Figure 7: *In-vitro* drug release pattern of BTZ, DL-HPBT PNPs, DL-HPLA PNPs and DL-HPLA-BT PNPs at pH (a) 7.4 (b) 5.6. Membrane dialysis method was followed for the release studies *in vitro.*

***Ex-vivo* hemolytic toxicity study**

Concentration dependent hemolysis toxicity analysis **(Figure 8)** was performed to determine the interaction of erythrocytes with BTZ and prepared formulations. BTZ displayed 24% hemolysis, whereas DL-HPLA-BT PNPs showed only 12% hemolysis against RBCs at a concentration of 150 µg/mL indicated that DL-HPLA-BT PNPs were 2-fold less toxic than BTZ with $p<0.0001$. Interestingly, the biotin anchored HPLA-PNPs (i.e. DL-HPLA-BT PNPs) showed less toxicity due to reduced interaction of nanoparticles with erythrocytes. In comparison of DL-HPLA-PNPs, the DL-HPBT PNPs exerted a minimal hemolytic toxicity on erythrocytes at similar concentration. At lower concentration of 10 µg/mL, a considerably decrease in hemolysis toxicity was noticed for DL-HPLA-BT PNPs than BTZ. The hemolytic toxicity for PNPs was 2-fold less than BTZ at 50 µg/mL, similarly 2-fold decrease was seen in case DL-HPBT PNPs than DL-HPLA PNPs. Peripheral neuropathy and thrombocytopenia are considered as dose limiting toxic effects of BTZ as per literature [8]. This is also one reason that the study was planned and conducted.

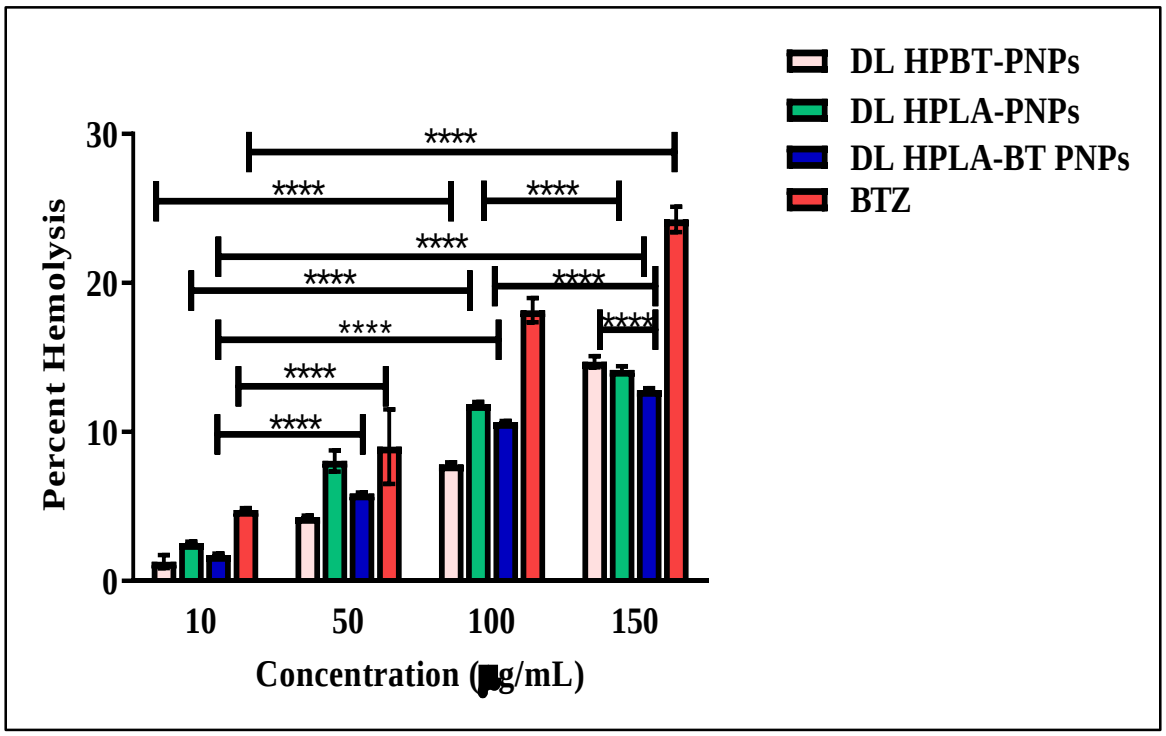

Figure 8: *Ex vivo* hemolysis of BTZ and drug loaded (DL) PNPs of HPBT, HPLA, HPLA-BT at different concentrations (10, 50,100,150 µg/mL); Values represents mean ± SD (n=3). **** $p<0.0001$ indicates the less significant differentiate between various concentrations of drug and drug loaded formulations (Two-way ANOVA; Bonferroni multiple comparisons test).

Cytotoxicity assay

Cytotoxicity of drug-loaded formulations was examined on MCF-7 breast cancer cell lines through MTT assay **(Figure 9 a)**. BTZ showed variable cytotoxicity against breast cancer cell line MCF-7 (IC_{50} = 100 ± 8.4 nM), MDA-MB-231 (IC_{50} = 7 ± 2.7 nM), MDA-MB-468 (IC_{50} = 5 ± 2.4 nM) MDA-MB- 453 (IC_{50} = 100 ± 12.1 nM) [37]. The IC_{50} values calculated for DL-HPBT-PNPs was 56.06 ± 0.12 nM, which was 1.97 (approximately 2-folds) less than BTZ with $p<0.0001$ as per the experimental results while blank PNPs of HPLA-BT were found to be non-toxic to MCF-7 cells. Results inferred that significant reduction in IC_{50} values were observed for biotin conjugated PNPs (DL-HP-BT PNPs and DL-HPLA-BT PNPs). However, significant reduction in IC_{50} values was not seen in case of DL-HPLA PNPs which indicates the role of biotin in ascertaining enhanced anticancer activity of biotin conjugated formulations against MCF-7 breast cancer cells. The biotinylated formulations acted efficiently than non-biotinylated one. The drug loaded PNPs (DL-HP-BT PNPs, DL-HPLA PNPs and DL-HPLA-BT PNPs) exhibited higher cytotoxicity at lower concentration of drug as compared to pure BTZ against MCF-7 breast cancer cells **(Figure 9 b)**. These results revealed that drug loaded PNPs possessed significant anti-cancer effect.

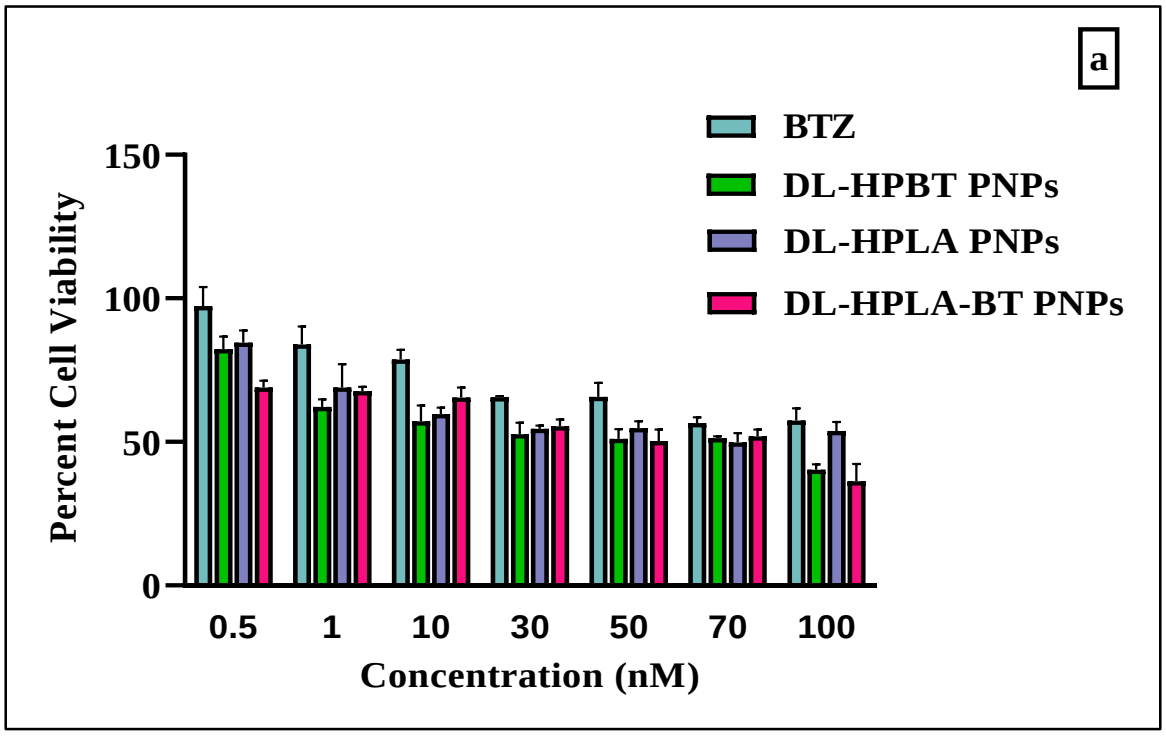

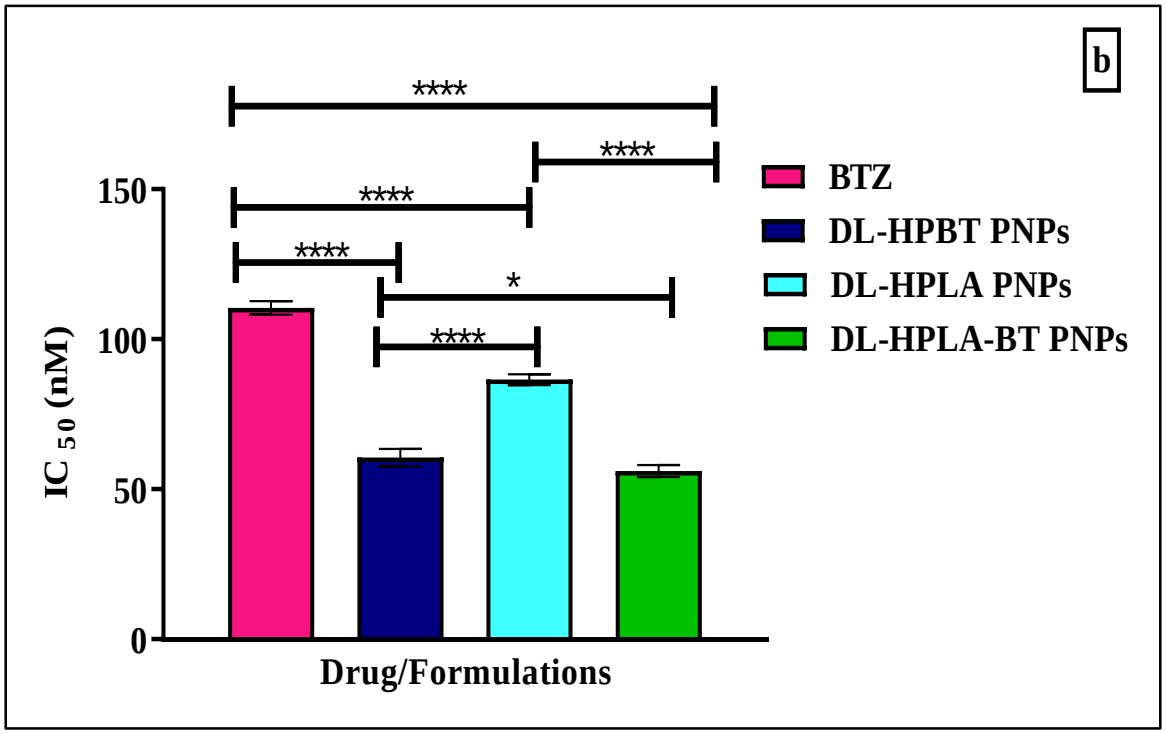

Figure 9: (a) Percent cell viability of BTZ and DL-HPBT PNPs, DL-HPLA PNPs and DL-HPLA-BT PNPs (b) IC_{50} of BTZ and DL-HPBT PNPs, DL-HPLA PNPs and DL-HPLA-BT PNPs. **** indicates the extremely significant difference with $p<0.0001$, while * indicates less significant difference with $p<0.05$ (Newman-Keuls multiple comparison test).

Cellular uptake study

The intracellular uptake of free BTZ and BTZ loaded formulations (DL-HPBT PNPs, DL-HPLA PNPs and DL-HPLA-BT PNPs) was investigated by fluorescence microscopy through FITC (fluorescence isothiocyanate) dye. Here, we used biotin which acts as a cell targeting molecule and can be taken up by tumor cells selectively as per reported literature [36]. Biotin receptors are overexpressed in cancerous cells and biotin can be used in tracking of tumor surface *via* prepared nanoparticles tagged with polymers as cargo [41]. Therefore, now-a-days targeting ligand-based therapeutics has become a choice of drug targeting that can directly enter into tumor cells/surface. From the results **(Figure 10)**, it was inferred that in 2 h, higher uptake of biotinylated PNPs than non-biotinylated HPLA-PNPs was observed. This may be due to the targeting potential of biotin attached to HPLA-BT PNPs. In the similar way, HPBT PNPs exhibited higher uptake than HPLA PNPs **(Figure 10)**. Higher uptake of drug loaded PNPs was observed in the cells in a time dependent manner. This plausible effect ensured more surface binding affinity of biotin to tumor

cells surface in case of HPLA-BT nanoparticles than non-biotinylated HPLA PNPs. Similarly, biotin conjugated HPMA PNPs (HPBT PNPs) showed less intensity than non-biotin conjugated HPLA-PNPs after 24 h. This may be due to the appropriate biotin tethering on the surface of HPLA-BT PNPs. From these findings, it was concluded that developed HPLA-BT PNPs could be used for effective breast cancer targeting using biotin as a ligand.

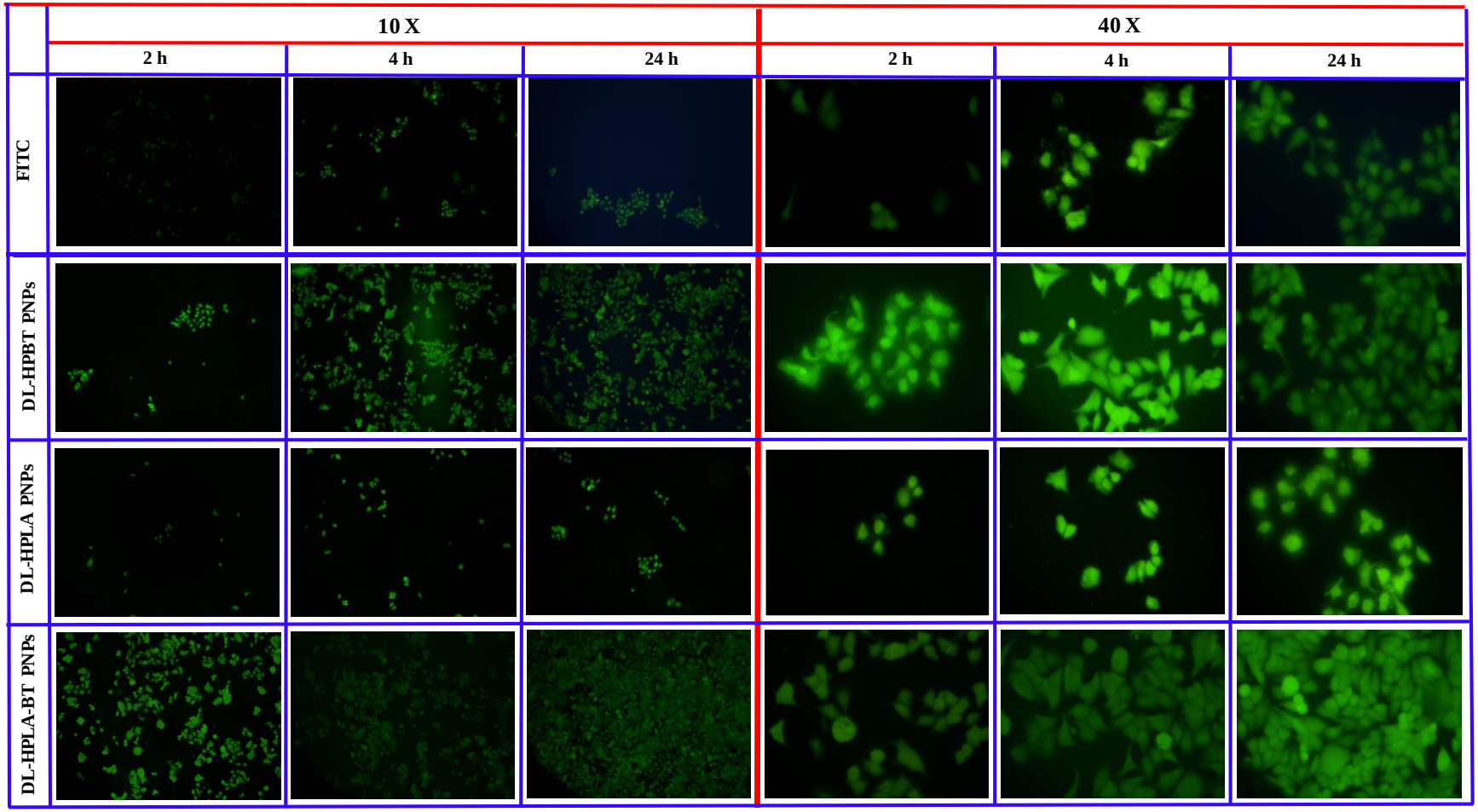

Figure 10: Cellular uptake study of (a) FITC (fluorescein isothiocyanate) as control; (b) DL-HPBT PNPs; (c) DL-HPLA PNPs; (d) DL-HPLA-BT PNPs performed against MCF-7, breast cancer cell line. Biotin conjugated formulation such as DL-HPBT PNPs, DL-HPLA-BT PNPs possessed robust cellular internalization except DL-HPLA PNPs formulation due to presence of biotin molecules suggesting that the cellular entry of FITC tagged formulations are mediated by biotin receptors present on the cell surface and the expression of these receptors is higher on cancerous cell surface than the non-cancerous cells.

In vivo pharmacokinetic study

The BTZ calibration curve was estimated via RP-HPLC method optimized by ACN: methanol: water (70: 30: 0.1) to obtain a sharp peak of drug as per the reported protocol [33] with a run time of 10 min. The positive and encouraging results obtained from *in vitro* release studies, cellular uptake, and cytotoxicity study impelled us for the *in vivo* pharmacokinetic studies in Sprague Dawley rats. Time dependent plasma drug concentration of BTZ, DL-HPBT PNPs, DL-HPLA PNPs, DL-HPLA-BT PNPs were plotted in **(Figure 11)**. The desired pharmacokinetic parameters were estimated by indicating the data into one compartmental open body (1 CBM) *i.v.* push/bolus model. The high elimination rate constant of drug and relatively low K values supports the intended objectives of the study. The elimination rate constant of DL-HPLA-BT PNPs was observed to be less than pure drug. The bioavailability ($AUC_{0-\infty}$) of DL-HPLA-BT PNPs was enhanced by 8.5 folds than BTZ. A reduction in V_d was calculated for DL-HPBT PNPs **(Table 2)**. The half-life of DL-HPLA-BT PNPs was increased by approximately 2.52 times than BTZ. The increase in bioavailability, half-life and decrease in clearance rate confirmed the increment in the retention time of the formulations. Overall, the pharmacokinetic study reflected the results obtained in *in vitro* release study. The higher retention time in terms of improved bioavailability is an indirect evidence of the sustained behavior of DL-HPLA-BT PNPs.

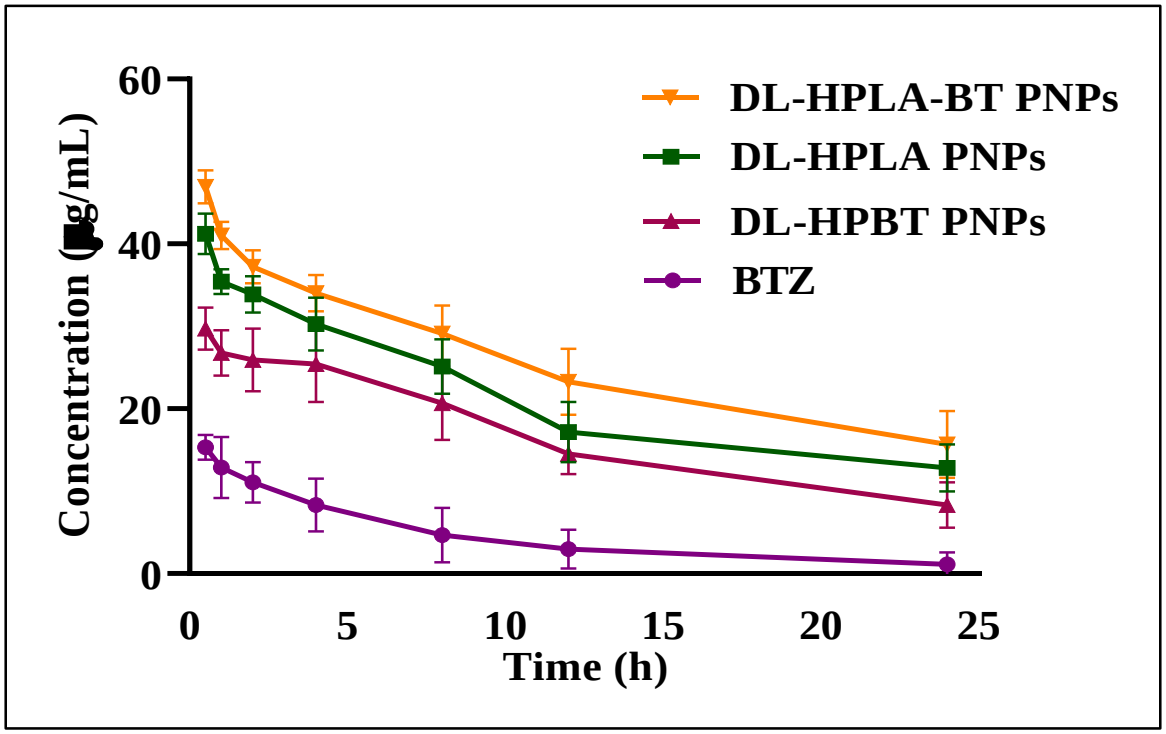

Figure 11: Plasma concentration-time profile of DL-HPLA-BT PNPs, DL-HPLA PNPs, DL-HPBT PNPs and BTZ obtained from *in vivo* pharmacokinetic study in Sprague-Dawley rats. Values represents mean ± SD (n=4).

Table 2: Pharmacokinetics Parameters of BTZ, DL-HPBT PNP, DL-HPLA PNPs and DL-HPLA-BT PNPs by Intravenous Administration in Sprague Dawley Rats. Values represent mean ± S.D, AUC = area under the curve, K(h) elimination rate constant, t1/2 = plasma half-life, Cl = clearance, Vd = volume of distribution.

PK Parameters	BTZ	DL-HPBT PNPs	DL-HPLA PNPs	DL-HPLA-BT PNPs
AUC $_{0\text{-}t}$ (µg mL^{-1} h^{-1})	102.74±0.28	391.60±0.022	493.21±0.01	596.95±0.15
AUC $_{0\text{-}\infty}$ (µg $mL^{-1}h^{-1}$)	112.90±0.32	546.27±0.02	755.38±0.021	955.51±0.23
k (h^{-1})	0.110±0.01	0.054±0.011	0.049±0.001	0.044±0.02
$t_{1/2}$ (h)	6.28±0.04	12.91±0.14	14.19±0.011	15.84±0.01
V_d (L)	18.65±0.024	8.40±0.02	6.70±0.24	5.90±0.31
Cl (L/h)	2.058±0.03	0.451±0.12	0.33±0.20	0.258±0.03

Statistical Analysis

All the results were expressed as triplet of mean ± SD. Two-way ANOVA and other tests (Newman-Keuls multiple comparison test, (Bonferroni multiple comparisons test).) were applied on the results of different experiment to minimize the errors.

Discussion

Developing and exploring newer polymers for the possible applications in drug delivery is bit challenge. Polymers have become the indispensable part of the drug delivery approaches. Polymers like PEG, PLA and PLGA have given immense opportunities for the biomedical scientists in better development of dosage forms and prodrugs. Exploring HPMA in the direction of polymer exploration is one of the mottos this research. The quest is to propose a polymer which can have multiple applications in biomedicals such as PEG or PLA has. HPMA does offer certain advantages which can be explored to claim its possibilities in drug delivery applications. In the recent past, we have attempted to successfully deliver anti-TB drugs (in multi-drug approach) using HPMA nanoparticles. In this study, we attempted to explore another facet of HPMA possibility for delivering anti-cancer drugs. This study is a mix of polymeric synthesis exhaustively supported by the extensive characterization as well as the exploration of the developed conjugates for the targeted delivery of BTZ. Polymeric conjugation is a complex and tedious process, but present attempt was successful in synthesizing and characterizing HPMA conjugates through the support of the spectroscopic techniques such as ^{1}H and ^{13}C NMR, FT-IR and UV-visible spectroscopy. In recent times, HPMA based drug encapsulation and conjugation research has entered in the clinical trials too. The characteristic properties of HPMA enforces to utilize it for improving BTZ delivery in breast cancer cells. HPMA-PLA (HPLA) block copolymers were synthesized following a mechanism relied on an active ester and amide functionality approach. Then, the polymeric conjugates were fabricated into PNPs by o/w emulsion method. The size of BTZ loaded HPLA-BT PNPs was found to be 199.7±1.32 nm with zeta potential of -3.20±0.22 and PDI of 0.196±0.11 and showed homogeneity. The obtained results can be clearly correlated with the effect of size and biotinylation. The cytotoxicity data is indicative to emphasize on significant aspects of HPMA over pure drug delivery. BTZ is relatively new molecule for establishing better strategy for its delivery. The present study is indicative that it can be successfully delivered with better outcome using HPMA based PNPs. The prepared PNPs were able to demonstrate the influence of polymeric conjugation in the form of nanoparticles to

investigate hemolytic toxicity, cytotoxicity, cellular uptake, and *in vivo* pharmacokinetics. The percent hemolysis data suggested that BTZ and BTZ loaded formulations showed concentration dependent hemolytic toxicity. At concentration of 150 µg/mL, BTZ showed maximum hemolytic toxicity, while BTZ loaded HPLA-BT PNPs were less hemolytic than the drug at the same concentration. It was also noticed in the previous literature that, BTZ exhibited hemolytic toxicity behavior as a side-effect of chemotherapy. The cell-line based study inferred that BTZ loaded PNPs were more cytotoxic than BTZ. From the cellular uptake studies, it was concluded that DL-HPLA-BT PNPs can enter into the MCF-7 breast cancer cells more efficiently than pure drug. The enhanced cellular uptake may be due to the biotinylation of HPMA in HPMA-BT and HPMA-PLA-BT polymeric conjugates. Biotin overexpression on receptors in breast cancer cells may be one of the reasons why the uptake was enhanced in case of biotinylated PNPs in comparison to non-biotinylated one. Of-course, the better outcome can be evaluated only with the *in vivo* studies performed in suitable breast cancer induced animal model, but we decided to carry out the *in vivo* studies first in normal healthy rats to get an profile of the plasma distribution pattern of the developed PNPs. Specific objective was to ensure, what kind of pharmacokinetic profile is displayed by the prepared PNPs. The obtained results were encouraging and supported the hypothesis that the prepared PNPs were able to exert the stealth nature as per as plasma drug concentration is concerned. Polymeric nanoparticles of BTZ were reported in the past but hitherto no one reported the biotin conjugated HPMA and PLA polymeric conjugates (HPLA-BT) and their modifications in to PNPs for BTZ delivery. In conclusion, HPMA co-polymer and its polymeric conjugates such as HPMA-Biotin/HP-BT, HPMA-PLA/HPLA, HPMA-PLA-Biotin/HPLA-BT were successfully conjugated which are being reported for the first time for targeted delivery of BTZ. Particularly, the BTZ loaded HPMA-PLA-Biotin/HPLA-BT polymeric nanoparticles showed high drug loading capacity and encapsulation efficiency within 200 nm size range. BTZ loaded HPLA-BT PNPs represented an attractive and innovative approach to improve the efficacy of BTZ for breast cancer therapy in targeted manner. The high drug loading capacity of PNPs have promising potential for BTZ against solid tumor. The prepared PNPs exhibited reduced hemolytic toxicity than BTZ in a concentration dependent study. The *in vitro* release studies suggested sustained and controlled release of drug at pH 7.4 however, faster drug release was observed at pH 5.6 (endosome). This suggested that the rate of release changes/depends on variant pH condition. The smart targeting moiety, biotin, successfully enhanced the internalization of BTZ loaded PNPs

such as HP-BT and HPLA-BT thereby improving the anti-cancer activity of BTZ. The cytotoxicity study also indicated the higher cytotoxic effects of DL-HPLA-BT PNPs on MCF-7 cell lines. The decrease in IC_{50} values for the prepared formulations supported the potential of biotin functionalized PNPs for breast cancer therapy. *In vivo* kinetics result revealed the increment in bioavailability and half-life of DL-HPLA-BT PNPs than pure drug which impelled that this approach may be beneficial for targeting breast cancer treatment if explored further. Although only few targeted drugs have been developed so far, this area is in constant growth and we strongly believe that this approach could give an added value to cancer chemotherapy therapy.

Impact of the research in the advancement of knowledge or benefit to mankind

I believe that the scientific exposure and the proposed research will represent an important component in the efforts for searching new effective ways of synthesis, preparation, and evaluation of polymer-based nanostructures to combat breast cancer. The developed formulation is with lesser side-effects and improving drug therapy using water soluble HPMA co-polymer. HPMA based nanotherapeutics are currently utilized for the sake of human health. HPMA has wide range of application in cancerous and non-cancerous diseases. Breast cancer is a disease frequently occurring in women globally therefore some, stride efforts are needed to develop for better management of breast cancer. The present work successfully targeted the breast cancer cell lines with a ligand, biotin and deliver BTZ at the action of site with great efficiency. The cellular uptake and pharmacokinetics results were also encouraging to explore this work to the next level in future. This work can be beneficial for humanity as it can be proved that co-polymeric NPs drug delivery can be an effective strategy to deliver hydrophobic anti-cancer drug BTZ. Additionally, use of HPMA as an established copolymer for controlled release and showed the potential for effective cancer therapy. Many of the HPMA based polymeric conjugates are currently in clinical trials. Developing a newer polymeric option in the form of HPMA can be challenge but if explored in right direction, it can be a remarkable option. This study gives a better option for biomedical scientists to overcome the chemotherapeutic hurdles of delivery of BTZ for the better treatment of cancer patients. We hope for the excellent outcomes in near future that will definitely reduce the burden of cancer.

Literature references

[1] H. Ringsdorf, Structure and Properties of Pharmacologically Active Polymers, Journal of Polymer Science: Polymer Symposia, 51 (1975) 135-153.
[2] P.A. Vasey, S.B. Kaye, R. Morrison, C. Twelves, P. Wilson, R. Duncan, A.H. Thomson, L.S. Murray, T.E. Hilditch, T. Murray, S. Burtles, D. Fraier, E. Frigerio, J. Cassidy, Phase I Clinical and Pharmacokinetic Study of PK1 [N-(2-Hydroxypropyl)Methacrylamide Copolymer Doxorubicin]: First Member of A New Class of Chemotherapeutic Agents-Drug-Polymer Conjugates. Cancer Research Campaign Phase I/II Committee. Clinical Cancer Research (1999) 83-94.
[3] S. Baka, A.R. Clamp, G. C. Jayson, A Review of the Latest Clinical Compounds to Inhibit VEGF In Pathological Angiogenesis, Expert Opinion on Therapeutic Targets, 10 (2006) 867-876.
[4] F. M. Veronese, G. Pasut, Pegylation, Successful Approach to Drug Delivery, Drug Discovery Today 10 (2005) 1451-1458.
[5] M. Elsabahy, K.L. Wooley, Design of Polymeric Nanoparticles for Biomedical Delivery Applications, Chemical Society Reviews, 41 (2012) 2545-2561.
[6] F. Bray, J. Ferlay, I. Soerjomataram, R.L. Siegel, L.A. Torre, A. Jemal, Global Cancer Statistics 2018: GLOBOCAN Estimates of Incidence and Mortality Worldwide for 36 Cancers in 185 Countries, CA: A Cancer Journal for Clinicians, 68 (2018) 394-424.
[7] S,T. Pearce, V.C. Jordan, The Biological Role of Estrogen Receptors Alpha and Beta in Cancer, Critical Reviews in Oncology/hematology, 50 (2004) 3-22.
[8] D. Chen, M. Frezza, S. Schmitt, J. Kanwar, Q.P. Dou, Bortezomib as the First Proteasome Inhibitor Anticancer Drug: Current Status and Future Perspectives, Current Cancer Drug Targets, 11 (2011) 239-253.
[9] C.N. Papandreou, D.D. Daliani, D. Nix, H. Yang, T. Madden, X. Wang, Phase I Trial of the Proteasome Inhibitor Bortezomib in Patients With Advanced Solid Tumors with Observations in Androgen-Independent Prostate Cancer, Journal of Clinical Oncology, 22 (2004) 2108-2121.
[10] M. Maynadier, I. Basile, A. Gallud, M. Gary-Bobo, M. Garcia, Combination Treatment with Proteasome Inhibitors and Antiestrogens has a Synergistic Effect Mediated by p21WAF1 in Estrogen Receptor-Positive Breast Cancer, Oncology Reports, 36 (2016) 1127-1134.
[11] S. Thaler, M. Schmidt, S. Robetawag, G. Thiede, A. Schad, J.P. Sleeman, Proteasome Inhibitors Prevent Bi-directional HER2/Estrogen-Receptor Cross-talk Leading to Cell Death in Endocrine and Lapatinib-resistant HER2+/ER+ Breast Cancer Cells, Oncotarget, 8 (2017) 72281-72301.
[12] X. Xia, Y. Liao, Z. Guo, Y. Li, L. Jiang, F. Zhang, H. Chuyi, L. Yuan, W. Xuejun, L. Ningning, L. Jinbao, H. Hongbiao, Targeting Roteasome-Associated Deubiquitinases as a Novel Strategy for the Treatment of Estrogen Receptor-Positive Breast Cancer, Oncogenesis, 7 (2018) 75.
[13] W. Wei, Z.G. Yue, J.B. Qu, H. Yue, Z.G. Su, G.H. Ma, Galactosylated Nanocrystallites of Insoluble Anticancer Drug for Liver-Targeting Therapy: an *In Vitro* Evaluation, Nanomedicine, 5 (2010) 589-596.

[14] J. Su, F. Chen, V.L. Cryns, P.B. Messersmith, Catechol Polymers for pH-Responsive, Targeted Drug Delivery to Cancer Cells, Journal of American Chemical Society, 133 (2011) 11850-53.
[15] S. Medel, Z. Syrova, L. Kovacik, J. Hrdy, M. Hornacek, E. Jager, M. Hruby, R. Lund, D. Cmarko, P. Stepanek, I. Raska, B. Nystromet, Curcumin-bortezomib loaded polymeric nanoparticles for synergistic cancer therapy, European Polymer Journal, 93 (2017) 116-131.
[16] R. Duncan, Development of HPMA Copolymer-Anticancer Conjugates: Clinical Experience and Lessons Learnt, Advanced Drug Delivery Reviews, 61 (2009), 1131-1148.
[17] L.W. Seymour, D.R. Ferry, D.J. Kerr, D. Rea, M. Whitlock, R. Poyner, C. Boivin, S. Hesslewood, C. Twelves, R, Blackie, A. Schatzlein, D. Jodrell, D. Bissett, H. Calvert, M. Lind, A. Robbins, S. Burtles, R. Duncan, J. Cassidy, Phase II studies of Polymer-Doxorubicin (PK1, FCE28068) in the Treatment of Breast, Lung and Colorectal Cancer, International Journal of Oncology, 34 (2009) 1629-1636.
[18] M. Barz, A. Arminan, F. Canal, F. Wolf, K. Koynov, H. Frey, P(HPMA)-block-P(LA) Copolymers in Paclitaxel Formulations: Polylactide Stereochemistry Controls Micellization, Cellular Uptake Kinetics, Intracellular Localization and Drug Efficiency, Journal of Controlled Release, 163 (2012) 63-74.
[19] J. Senior, J.C. Crawley, G. Gregoriadis, G. Tissue Distribution of Liposomes Exhibiting Long Half-Lives in the Circulation after Intravenous Injection, Biochimica Biophysica Acta. 839 (1985) 1-8.
[20] S. Maiti, N. Park, J.H. Han, H.M. Jeon, J.H. Lee, S. Bhuniya, Gemcitabine–Coumarin–Biotin Conjugates: A Target Specific Theranostic Anticancer Prodrug, Journal of American Chemical Society, 135(2013) 4567-4572.
[21] C.S. Kue, A. Kamkaew, K. Burgess, L.V. Kiew, L.Y. Chung, H.B. Lee, Small Molecules for Active Targeting in Cancer, Medicinal Research Review, 36 (2016) 494-575.
[22] W.X. Ren, J. Han, S. Uhm, Y.J. Jang, C. Kang, J.H. Kim, J.S. Kim, Recent Development of Biotin Conjugation in Biological Imaging, Sensing, and Target Delivery, Chemical Communications, 51(2015) 10403-10418.
[23] S. Shen, D. Xiao-Jiao, J. Liu, S. Rong, Y.H. Zhu, J. Wang, Delivery of bortezomib with nanoparticles for basal-like triple-negative breast cancer therapy, Journal of Controlled Release, 8 (2015)14-24.
[24] P. Chytil, T. Etrych, J. Kriz, V. Subr, K. Ulbrich K, N-(2-Hydroxypropyl)methacrylamide-Based Polymer Conjugates with pH-Controlled Activation of Doxorubicin for Cell-Specific or Passive Tumour Targeting Synthesis by RAFT Polymerisation and Physicochemical Characterisation, European Journal of Pharmaceutical Sciences, 41 (2010) 473-482.
[25] S. Upadhyay, I. Khan, A. Gothwal, P.K. Pachouri, N. Bhaskar, U.D. Gupta, Conjugated and Entrapped HPMA-PLA Nano-Polymeric Micelles Based Dual Delivery of First Line Anti TB Drugs: Improved and Safe Drug Delivery against Sensitive and Resistant Mycobacterium Tuberculosis, Pharmaceutical Research, 34 (2017) 1944-1955.

[26] X. Hou, W. Wei, Y. Fan, J. Zhang, N. Zhu, H. Hong, Study on Synthesis and Bioactivity of Biotinylated Emodin, Applied Microbiology and Biotechnology, 101 (2017) 5259-5266.
[27] J.D. Goodreid, P.A. Duspara, C. Bosch, R.A. Batey, Amidation Reactions from the Direct Coupling of Metal Carboxylate Salts with Amines, Journal of Organic Chemistry, 79 (2014) 943-954.
[28] M. Getlik, B.J. Wilson, M.M. Morshed, I.D.G. Watson, D. Tang, P. Subramanian, Rearrangement of 4-Amino-3-halo-pyridines by Nucleophilic Aromatic Substitution, Journal of Organic Chemistry, 78 (2013) 5705-5710.
[29] P. Prabu, A.A Chaudhari, N. Dharmaraj, M.S. Khil, S. Park, H.Y. Kim, Preparation, Characterization, *In-Vitro* Drug Release and Cellular Uptake of Poly(Caprolactone) Grafted Dextran Copolymeric Nanoparticles Loaded with Anticancer Drug, Journal of Biomedical Materials Research Part A, 90 (2009) 1128-1136.
[30] I.D. Rosca, F. Watari, M. Uo, Microparticle Formation and its Mechanism in Single and Double Emulsion Solvent Evaporation, Journal of Controlled Release, 99 (2004) 271-280.
[31] R.B. Kumar, and S.T. Rao, AFM Studies on Surface Morphology, Topography and Texture of Nanostructured Zinc Aluminum Oxide Thin Films, Journal of Nano-materials and Biostructures, 7 (2012) 1881-1889.
[32] S.R. Byrn, P.A.Tishmack, M.J. Milton, H. Van de Velde, Analysis of Two Commercially Available Bortezomib Products: Differences in Assay of Active Agent and Impurity Profile, AAPS Pharmaceutical Science and Technology, 12 (2011) 461-467.
[33] Z. Kamalzadeh, E. Babanezhad, S. Ghaffari,A. Mohseni-Ezhiyeh, M. Mohammadnejad, M. Naghibfar, M. Bararjanian, H. Attar, Determination of Bortezomib in API Samples Using HPLC: Assessment of Enantiomeric and Diastereomeric Impurities, Journal of Chromatographic Science, 55 (2017) 697-705.
[34] A. Gupta, A. Ahmad, H. Singh, S.K.M.N. Kaur, M.M. Ansari, Nanocarrier Composed of Magnetite Core Coated with Three Polymeric Shells Mediates LCS-1 Delivery for Synthetic Lethal Therapy of BLM-Defective Colorectal Cancer Cells, Biomacromolecules, 19 (2018) 803-815.
[35] J. Codony-Servat, M.A. Tapia, M. Bosch, C. Oliva, J. Domingo-Domenech, B. Mellado, Differential cellular and molecular effects of bortezomib, a proteasome inhibitor, in human breast cancer cells, Molecular Cancer Therapeutics, 5 (2006) 665-675.
[36] W. Yang, Y. Cheng, T. Xu, X. Wang, L.P. Wen, Targeting cancer cells with biotin-dendrimer conjugates, European Journal of Medicinal Chemistry, 44 (2009) 862-868.
[37] A. Doerflinger, N.N. Quang, E. Gravel, G. Pinna, M. Vandamme, F. Duconge, Biotin-functionalized targeted polydiacetylene micelles, Chemical Communications, 54 (2018) 3613-3616.
[38] J. Nie, W. Cheng, Y. Peng, L. Liu, Y. Chen, X. Wang, C. Liang, W. Tao, Y. Wei, X. Zeng, L. Mei, Co-delivery of Docetaxel and Bortezomib Based on a Targeting Nanoplatform for Enhancing Cancer Chemotherapy Effects, Drug Delivery, 24 (2017) 1124-1138.

[39] V. Torchilin, Tumor Delivery of Macromolecular Drugs Based on the EPR Effect, Advanced Drug Delivery Reviews 63, (2011) 131-135
[40] Y. Singh, K.K.D.R. Viswanadham, V.K. Pawar, J. Meher, A.K. Jajoriya, A. Omer, S. Jaiswal, J. Dewangan, H.K. Bora, P. Singh, S.K. Rath, L. Jawahar, D.P. Mishra, M.K. Chourasia, M.K. Induction of Mitochondrial Cell Death and Reversal of Anticancer Drug Resistance via Nanocarriers Composed of a Triphenylphosphonium Derivative of Tocopheryl Polyethylene Glycol Succinate, Molecular Pharmaceutics (2019). DOI 10.1021/acs.molpharmaceut.9b00177.
[41] J.G. Vineberg, E.S. Zuniga, A. Kamath, Y.J. Chen, J.D. Seitz, I. Ojima, Design, Synthesis, and Biological Evaluations of Tumor-Targeting Dual-Warhead Conjugates for a Taxoid−Camptothecin Combination Chemotherapy, Journal of Medicinal Chemistry, 57 (2014) 5777−5791.